20

Electrospinning Fabrication and Characterization of Water Soluble Polymer/Montmorillonite/Silver Nanocomposite Nanofibers out of Aqueous Solution

Jeong Hyun Yeum[1], Jae Hyeung Park[1], In Kyo Kim[1] and In Woo Cheong[2]
[1]*Department of Advanced Organic Materials Science & Engineering, Kyungpook National University, Daegu 702-701*
[2]*Department of Applied Chemistry, Kyungpook National University, Daegu 702-701 Korea*

1. Introduction

Polymer nanocomposites are a class of materials that have properties that offer significant commercial potential. It was commonly defined as the combination of a polymer matrix resin and inclusions that have at least one dimension (i.e. length, width, or thickness) in the nanometer size range. There are many types of nanocomposites that have received significant research and development including polymer/inorganic particle, polymer/polymer, metal/ceramic, and inorganic based nanocomposites. These polymer hybrid nanocomposites have attracted great interest due to inorganic materials filled polymer composites often exhibit remarkable improvement in material properties with only a low percentage of inorganic materials. High degrees of stiffness, strength, conductivity and thermal resistance, etc. are realized with far less high density inorganic material, they are much lighter compared to conventional polymer composites. Many novel nanocomposites with improved performance properties, which may have large potential applications in the fields such as optics, electrical devices, and photoconductors were reported (Fleming et al., 2001; Luna-Xavier et al., 2001; Tiarks et al., 2001).

The synthesis of polymer nanocomposites is normally carried out by the following methods. One is based on in-situ polymerization of monomers inside the galleries of the inorganic host (Messersmith & Giannelis, 1993). The other approach is based on melt intercalation of polymers and it involves annealing a mixture of the polymer and the inorganic host, statically or under shear, above the T_g of the polymer (Usuki et al., 1997; Vaia et al., 1995). The solventless melt intercalation is an environmentally friendly technique and is adoptable to existing processing like roll milling, extrusion and molding. The materials made via these two processes have been summarized. Other unique methods for blending polymers directly with inorganic materials have employed microwaves, latex-colloid interaction, solvent evaporation, spray drying, spraying a polymer solution through a small orifice and Shirasu Porous Glass (SPG) membrane emulsification technique (Berkland et al., 2001; Fischer et al., 1999; Mu & Feng, 2001; Oriakhi & Lerner, 1995; Rosca et al., 2004).

The other techniques for preparing polymer nanocomposites is electrospinning process that has attracted great interest among academic and industrial scientists because it is very simple, low cost, and effective technology to produce polymer nanocomposite nanofibers which has been exhibit outstanding properties such as a high specific surface area and high porosity. These nanofibers can be used for a wide variety of applications such as separation filters, wound dressing materials, tissue scaffold, sensors, protective clothing, catalysis reaction, etc. (Choi et al., 2004; Han et al., 2006; Huang et al., 2003; Li & Xia, 2004; Reneker & Chun, 1996; Wang et al., 2002; Wu et al., 2005; Zussmas et al., 2003). Biomedical field is one of the important application areas. By utilizing electrospinning technique this field can be enriched widely. Different group have reviewed recently the patents and worked on electrospun biomedical nanostructures like tissue engineering, drug delivery and scaffold engineering (Min et al., 2004; Sangamesh et al., 2008; Vasita & Katti, 2006). In a typical electrospinning process, a high voltage is applied to a polymer fluid such that charges are induced within the fluid. When charges within the fluid reached a critical amount, a fluid jet will erupt from the droplet at the tip of the needle resulting in the formation of a Taylor cone. The electrospinning jet will travel towards the region of lower potential, which in most cases, is a grounded collector. There are many parameters that will influence the morphology of the resultant electrospun fibers, from beaded fibers to fibers with pores on its surface. The parameters affecting electrospinning and the fibers mat are broadly classified into polymer solution parameters, processing conditions which include the applied voltage, temperature and effect of collector, and ambient conditions. With the understanding of these parameters, it is possible to create nanofiber with different morphology by varying parameters.

Here, we have been fabricated several electrospun nanocomposite nanofibers in aqueous solutions with poly(vinyl alcohol) (PVA), chitosan oligosaccharide (COS), and pullulan (PULL) as polymer matrixs, and montmorillonite (MMT) and silver(Ag) nanoparticles as inorganic materials. The effectiveness of these nanocomposite nanofibers are demonstrated with a field emission-type scanning electron microscope (FE-SEM), a transmission electron microscopy (TEM), a reflection type X-ray diffraction (XRD), Fourier transform spectroscopy (FT-IR), Thermogravimetric analysis (TGA), differential scanning calorimeters (DSC) and the anti-bacterial performance was also discussed.

2. Background

MMT is one of the most useful inorganic material for nanocomposite, it has attracted great interest due to MMT filled polymer nanocomposites often exhibit remarkable improvement in material properties such as mechanical, thermal, flame-retardant, and barrier properties with only a low percentage of MMT fillers added. These property improvements are attributed to the nanometric thickness and high aspect ratio of the individual clay platelets, as well as to the nanocomposite morphology with the platelets being exfoliated and well-dispersed (Gates et al., 2000; Svensson et al., 2010).

Ag nanoparticles are widely used as a photosensitive components, catalysts and chemical analysis. Additionally, due to its comparatively high safety, many researchers have successfully developed antibacterial and disinfectant agents with silver composite using various polymers. Microorganisms with resistance to the antimicrobial activity of Ag are exceedingly rare. Such silver has a size of nano-level, the total surface area of the silver become larger in identity volume and antibacterial efficiency is increased (Glaus et al., 2002; Rujitanaroj et al., 2008).

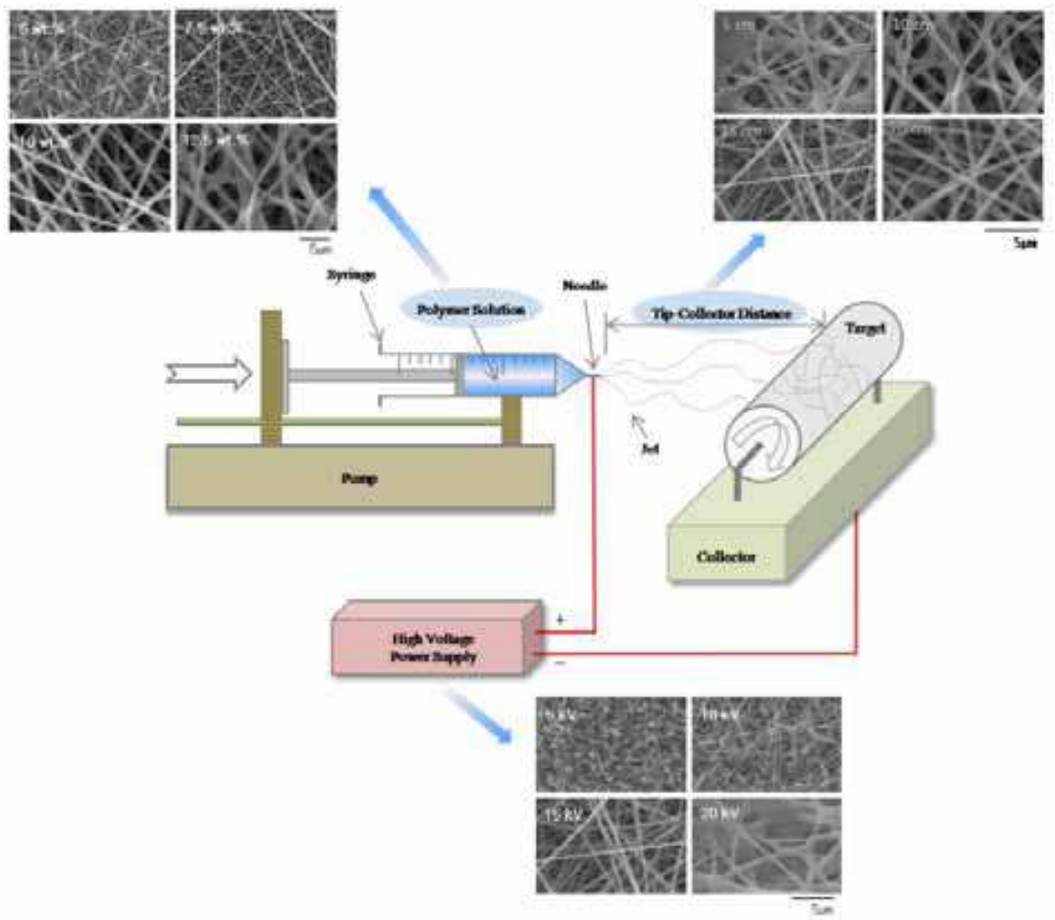

Fig. 1. Schematic representation of polymer/MMT nanocomposites

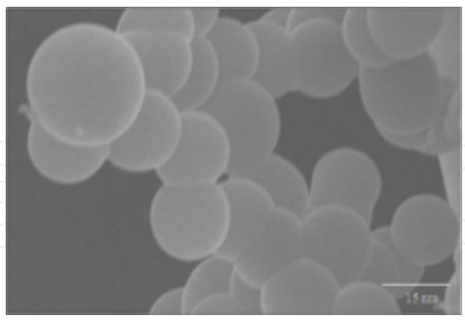

Fig. 2. SEM photograph of Ag nanoparticles

PVA is a semi-crystalline hydrophilic polymer with good chemical and thermal stability. Also, it has highly biocompatible and non-toxic. It can be processed easily and has high water permeability. These properties have led to the use of PVA in a wide range of applications in medical, cosmetic, food, pharmaceutical, and packaging industries. Especially, PVA has been used in fiber and film products for many years. Ultrafine PVA fibers, which may have different potential applications than microfibers, cannot be produced by conventional spinning techniques (Yeum et al., 2004).

Chitosan, the second most abundant polysaccharide in nature after cellulose, is an N-deacetylated derivative of chitin. It is generally regarded as non-toxic, biocompatible and biodegradable. It has many unique functional properties for different applications like high molecular weight, high viscosity, high crystallinity and capacity to hydrogen bond intermolecularly. However, the rigid D-glucosamine structure and high crystallinity in chitosan usually lead to poor solubility of chitosan in common organic solvents as well as in water, such as at physiological pH values (7.2–7.4), restricting its uses, especially in human body. However, partially depolymerized chitosan products, i.e., low molecular weight chitosan (COS), could overcome these limitations and hence find much wider applications in diversified fields (Kumar et al., 2004).

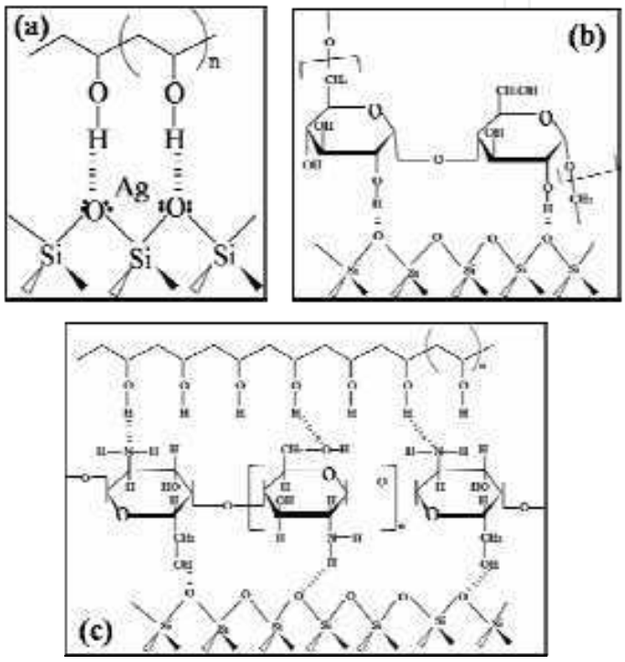

Fig. 3. Schematic representation of interaction(a) PVA/MMT/Ag, (b) PULL/MMT and (c) PVA/COS/MMT nanocomposite nanofibers

PULL is an extracellular microbial polysaccharide produced by the fungus-like yeast, Aureobasidium Pullulans (Yuen, 1974). It is a polysaccharide polymer consisting of maltotriose units, also known as α-1,4- ; α-1,6-glucan. Three glucose units in maltotriose are connected by an α-1,4 glycosidic bond, whereas consecutive maltotriose units are connected to each other by an α-1,6 glycosidic bond. The regular alternation of (1→4) and (1→6) bonds results in two distinctive properties of structural flexibility and enhanced solubility (Leathers, 1993). The unique linkage pattern also endows PULL with distinctive physical traits along with adhesive properties and its capacity to form fibers, compression moldings, and strong, oxygen impermeable films. Due to its excellent properties, PULL is used as a low-calorie ingredient in foods, gelling agent, coating and packaging material for food and drugs, binder for fertilizers and as an oxidation-prevention agent for tablets. Other applications include contact lenses manufacturing, biodegradable foil, plywood, water solubility enhancer and for enhanced oil recovery (Israilides, 1998; Leathers, 2003; Schuster, 1993). It is water soluble, insoluble in organic solvents and non-hygroscopic in nature. Its

aqueous solutions are stable and show a relatively low viscosity as compared to other polysaccharides. It decomposes at 250–280 °C. It is moldable and spinnable, being a good adhesive and binder. It is also non-toxic, edible, and biodegradable.

3. Experimental

3.1 Materials

PVA with P_n (number-average degree of polymerization) = 1700 [fully hydrolyzed, degree of saponification (DS)=99.9%] was obtained from DC Chemical Co., Seoul, Korea. COS (Average molecular weight above 10,000; 100% water soluble) was purchased from Kittolife Co., Kyongki-do, Korea and used without further purification. PULL was a food grade preparation (PF-20 grade) from Hayashibara Biochemical Laboratories Inc. (Okayama, Japan). MMT was purchased from Kunimine Industries Co. Ltd., Japan and aqueous Ag nanoparticle dispersion (AGS-WP001, 10,000 ppm) with diameters ca.15-30 nm was got from Miji Tech., Korea. Doubly distilled water was used as a solvent to prepare all solutions.

3.2 Electrospinning nanocomposite nanofibers

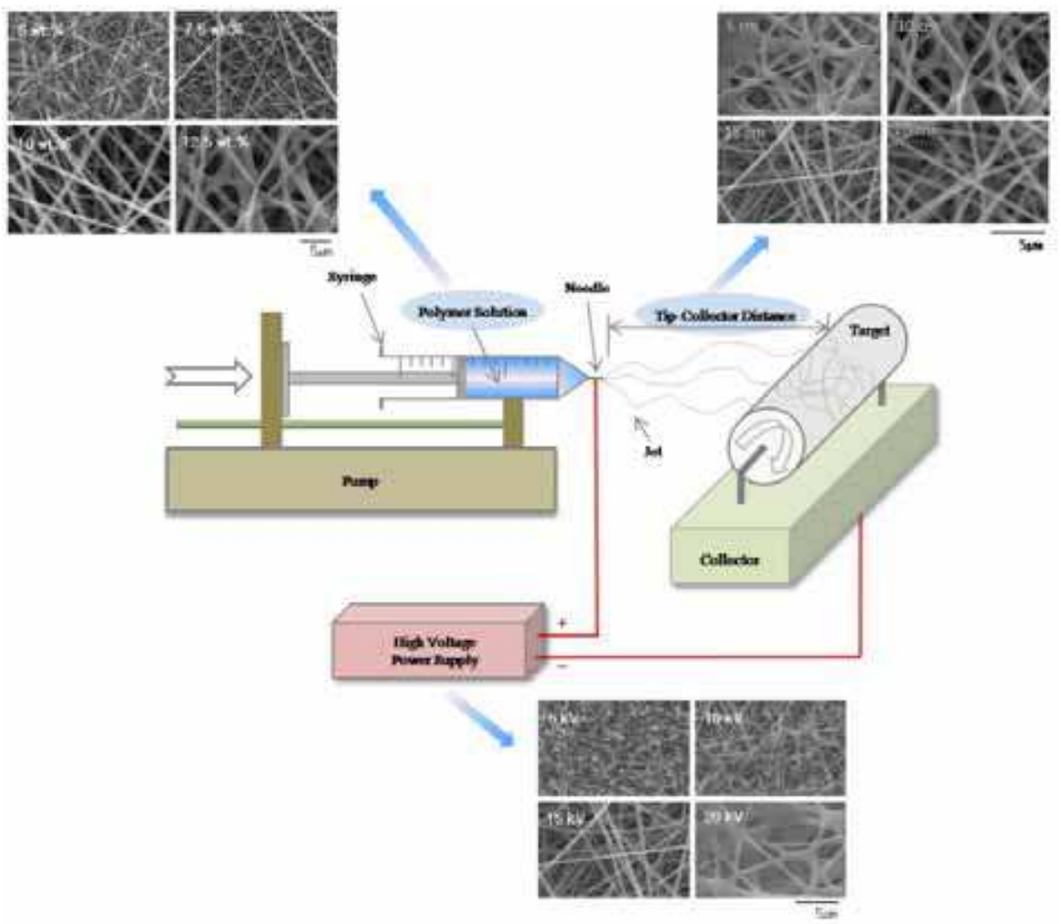

Fig. 4. Schematic representation of the electrospinning process and SEM image of PVA nanofibers at different conditions

During electrospinning, a high voltage power (CHUNGPA EMT Co., Korea) was applied to the polymer/inorganic material blend solution contained in a syringe via an alligator clip attached to the syringe needle. The applied voltage was adjusted at 15 kV. The solution was delivered to the blunt needle tip via syringe pump to control the solution flow rate. Fibers were collected on an electrically grounded aluminum foil placed at 15 cm vertical distance to the needle tip (Tip-Collector Distance, TCD). The above spinning conditions were found being the best condition to make PVA based nanofibers in our previous report (Ji et al., 2009; Karim et al., 2009; Lee et al., 2009a; Lee et al., 2009b; Park et al., 2009; Park et al., 2010).

Nanocomposite nanofiber		Total polymer concentration	Blend ratios	Contents*	
				MMT	Ag
Two types inorganic material	PVA	7.5 wt.%	-	-	-
	PVA/MMT			5 wt.%	
	PVA/MMT/Ag			5 wt.%	5 wt.%
Two types polymer	PVA/COS	12.5 wt.%	6/4	-	-
			8/2		
			10/0		
	PVA/COS/MMT		6/4	5 wt.%	
			8/2		
			10/0		
Natural polymer	PULL/MMT	20 wt.%	-	1 wt.%	
				3 wt.%	
				5 wt.%	
				10 wt.%	

* based on total polymer concentration

Table 1. Experimental condition for the preparation of nanocomposite nanofibers

4. Results and discussion

4.1 PVA/MMT/Ag nanocomposite nanofibers

4.1.1 Morphology and structure property

Figure 5 demonstrates FE-SEM and TEM images of PVA, PVA/MMT and PVA/MMT/Ag nanofibers electrospun with 5 wt.% of MMT and 5 wt.% of Ag nanoparticles. MMT contents were important parameters which had effects on the morphology of electrospun PVA nanofibers. The diameter of nanofibers increases but fibers homogeneity decreases with MMT contents. In the TEM image, the size of the dark line is about 1–3nm in width and 100–200nm in length, indicating the good dispersion and exfoliation of MMT layers in the nanofibers. This clearly indicates the feasibility of electrospinning of the 2-D platelet structures and the potential to achieve proper alignment of these clays along the fiber axis, which is critical for nanocomposite fiber fabrication. The Ag nanoparticles distribution along

the fiber direction and on the fiber cross-section is detected by TEM. It is seen that the MMT and Ag nanoparticles are distributed uniformly in nanofibers.

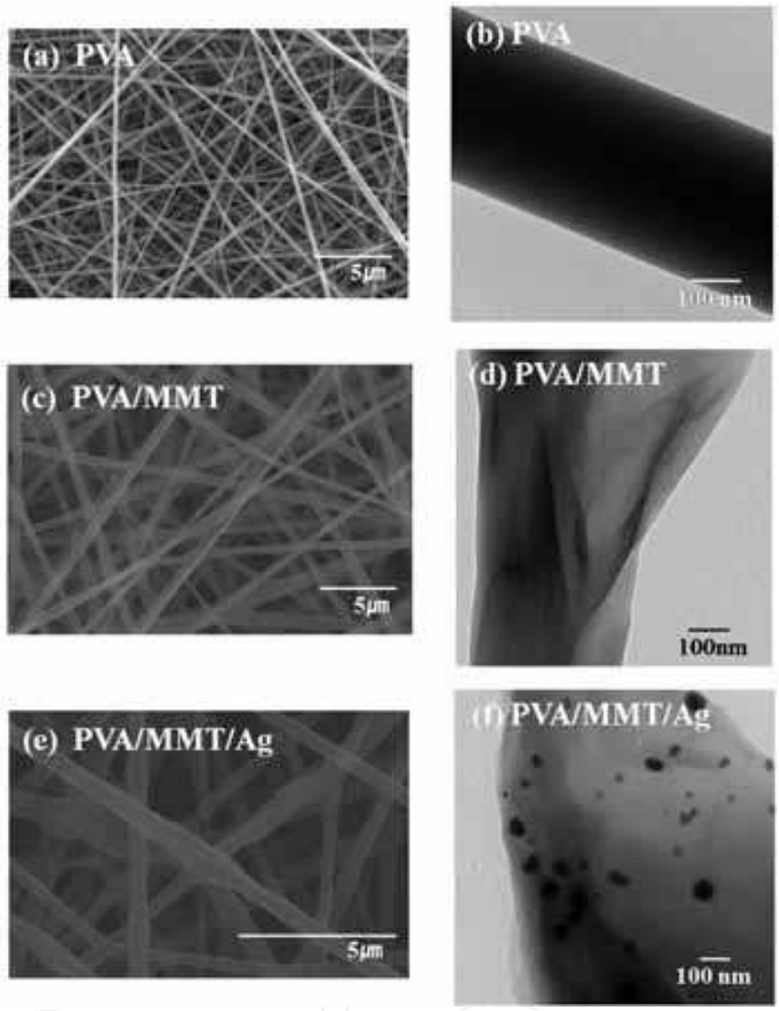

Fig. 5. FE-SEM and TEM images of (a), (b) pure PVA, (c), (d) PVA/MMT, (e), (f) PVA/MMT/Ag nanocomposite nanofibers

The XRD pattern (Fig. 6) of PVA/MMT/Ag nanocomposite nanofibers show diffraction peaks at 2θ of ca. 19.3° 38.2° and 44.6°, respectively [Fig. 6(c-e)]. The pure PVA nanofibers show a significant crystalline peak at about 19.3°, which is because of the occurrence of string inter- and intramolecular hydrogen bonding (Fig. 6a). In case of a clay-polymer composite, unexfoliated or intercalated MMT usually show a peak in the range 3~9° (2θ) (Fig. 16). In exfoliated nanocomposites, generally single silicate layers (1-3 nm thick) are homogeneously dispersed in the polymer matrix, and XRD patterns with no distinct diffraction peak in the range of 3~9° (2θ) could be observed (Fig. 6b) (Barber et al., 2005; Zhu et al., 2007). Except the diffraction peaks of PVA, all the other peaks are corresponding to the silver phase [Fig. 6 (c-e)]. The peaks of Ag are enlarged with increasing the content of Ag nanoparticles and crystallinity of PVA/MMT (2θ =19.3°) is lower in comparison with Figure 6b. These peaks are corresponding to the 111 and 200 planes of the silver nanocrystals with

cubic symmetry. XRD results indicate that MMT and Ag particles are well dispersed in the PVA nanofibers and MMT is predominantly exfoliated. TEM images further confirm MMT (Fig. 5d) and Ag nanoparticles (Fig. 5f) in the PVA/MMT/Ag nanocomposite nanofibers.

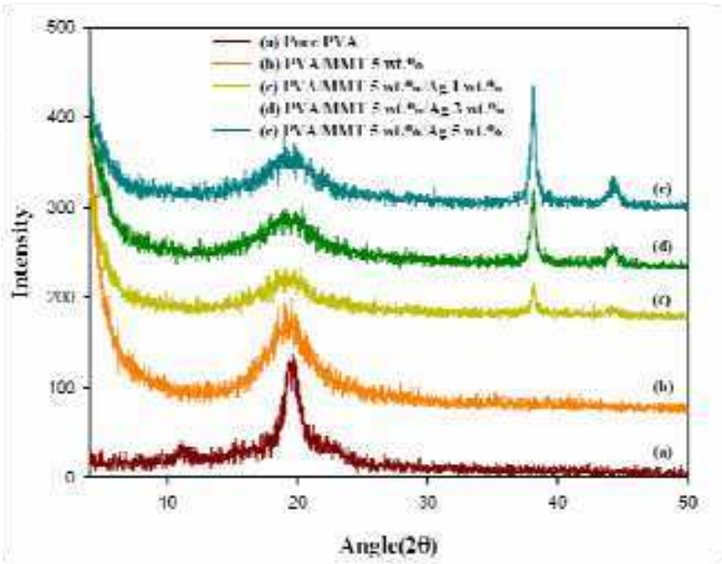

Fig. 6. XRD data of PVA/MMT/Ag nanocomposite nanofibers prepared with different Ag contents of 0 wt.%, 1 wt.%, 3 wt.% and 5 wt.%

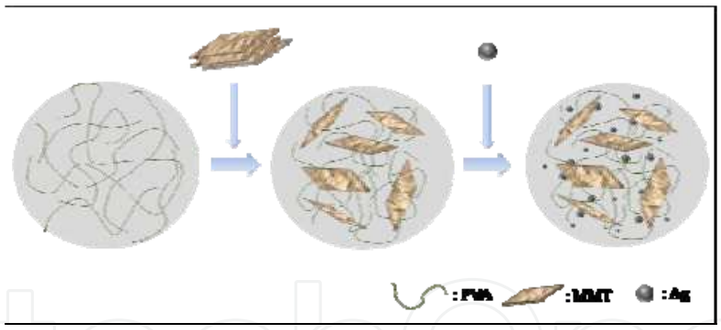

Fig. 7. Schematic representation of PVA/MMT/Ag nanocomposits

4.1.2 Thermal stability

Thermal stability of electrospun PVA, PVA/MMT and PVA/MMT/Ag nanofibers were measured using TGA in nitrogen atmosphere. Figure 8 shows TGA thermograms of different decomposition temperature with MMT and Ag contents. The most below curve of the TGA data (Fig. 8a) represent the pure PVA and the most upper curve (Fig. 8e) is for mass ratio of 5 wt.% of Ag nanoparticles i.e. the highest mass ratio of Ag contents is used in our work. Generally, when PVA is pyrolyzed in the absence of oxygen, it undergoes dehydration and depolymerization at temperature over 200 °C and 400 °C, respectively. The actual depolymerization temperature depends on the detail structure, molecular weight and conformation of the polymer. Figure 8(c, d) are displaying the middle masses ratio of Ag contents at the same trend of thermal stability like the Figure 8(a, e). Within up to 225 °C,

there is increased in thermal stability from the pure PVA nanofibers to PVA/MMT/Ag nanofibers. The higher thermal stability of high MMT and Ag content rate might be attributed to its higher chain compactness due to the interaction between the PVA, MMT and Ag nanoparticles.

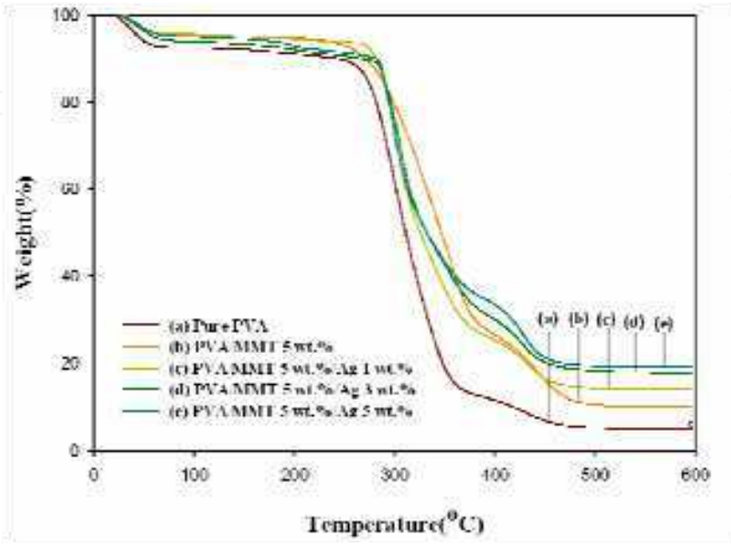

Fig. 8. TGA data of pure PVA nanofibers and PVA/MMT/Ag nanocomposite nanofibers prepared with different Ag contents of 0 wt.%, 1 wt.%, 3 wt.% and 5 wt.%

4.1.3 Anti-bacterial efficacy

The preservation efficacy for the PVA/MMT/Ag nanofiber was tested to evaluate the antimicrobial property (Farrington, 1994). Samples were prepared by dispersing the nanofibers in a viscous aqueous solution containing 0.01 wt.% of neutralized polyacrylic

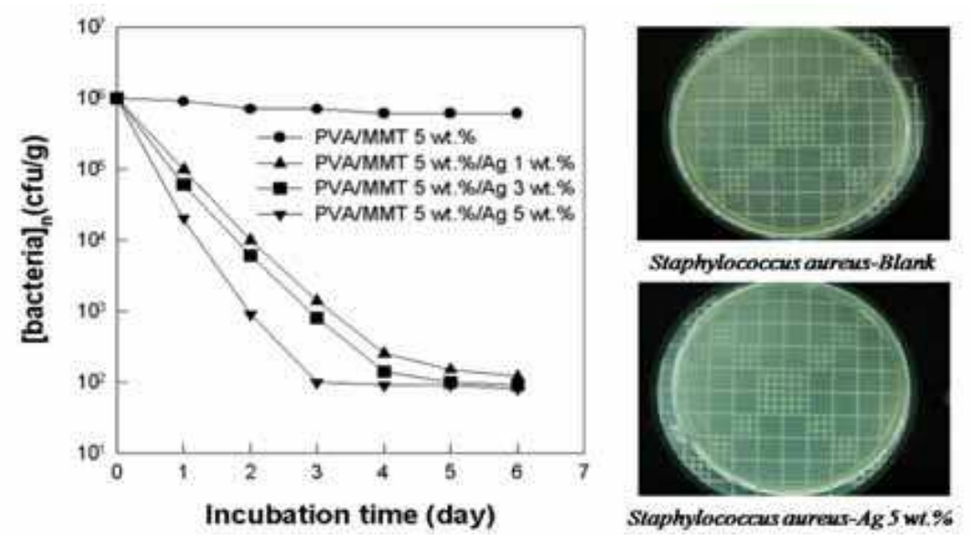

Fig. 9. Preservation performance of PVA/MMT/Ag nanocomposite nanofibers prepared with different Ag contents of 0 wt.%, 1 wt.%, 3 wt.% and 5 wt.%

acid (Carbopol 941, Noveon Inc.). A mixed culture of microorganisms, *Staphylococcus aureus* (ATCC6538), and *Escherichia coli* (ATCC25922) were obtained on tryptone soya broth after 24h incubation at 32 °C. Then, 20g of samples were inoculated with 0.2g of the microorganism suspensions to adjust the initial concentration of bacteria to 107 cfu/g. Then, the inoculant mixed homogeneously with the samples and was stored at 32 °C. The microbial counts were carried out using the pour plate count method.

As shown in Figure 9, the PVA/MMT/Ag nanofibers without Ag fail to have the anti-bacterial performance. The number of bacteria in the test samples remains constant for a long time. On the contrary, the incorporation of the PVA/MMT/Ag nanofibers into the test samples result in a remarkable decrease in the number of bacteria. The increase in the concentration of the Ag nanoparticles in nanofibers accelerates diminishing in bacteria. With only a small amount of Ag, almost all the initially inoculated bacteria could be sterilized within a week. This indicates that the PVA/MMT/Ag nanofibers have an anti-bacterial activity.

4.2 PVA/COS/MMT nanocomposite nanofibers

4.2.1 Morphology and structure property

Changing the polymer mass ratio of PVA/COS and the MMT content in the composite could alter the fiber diameter and morphology very effectively, as show in Figure 10. At the

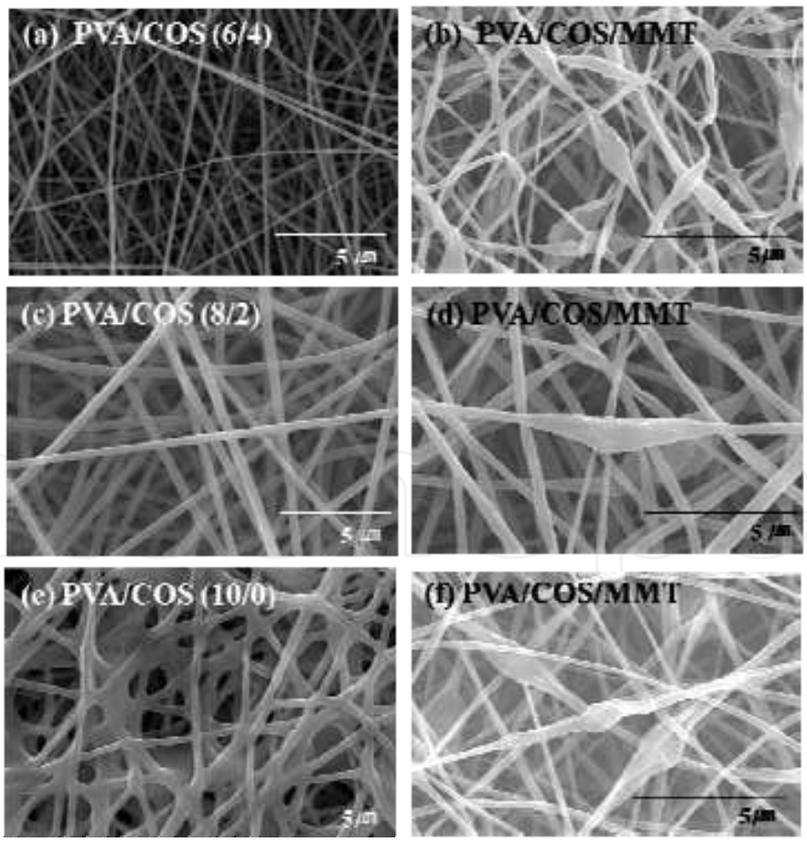

Fig. 10. FE-SEM images of PVA/COS and PVA/COS/MMT nanocomposite nanofibers prepared with different polymer blend ratios (MMT 5wt.%)

operation voltage of 15kV and tip to collector distance of 15cm, a series of nanofibers was made at a fixed total solid content (12.5 wt.%) but various PVA/COS mass ratio (6/4, 8/2 and 10/0) and 5 wt.% MMT contents (based on the total solid content). It should be noted that, when the PVA/COS mass ratio in the blend solutions is higher than 6/4, the viscosity of the solution is too low to be electrospun.

Figures 10 shows dramatic morphological changes as the mass of COS and concentration of MMT. By carefully comparing the SEM images shown in Figure 10, we found that fiber diameter show opposite tendency by COS ratio. It is known that the diameter of fibers and the formation of beads are strongly influenced by the viscoelasticity of the solution (Fong et al., 1999). Uniform nanofibers with diameters of 200-400 nm were obtained and no any beads were observed for PVA/COS ratios of 6/4 and 8/2. It was also noticed that the fiber diameter of PVA/COS is ~200 nm at a PVA/COS mass ratio of 6/4, which is much smaller than the diameter of fibers obtained at a PVA/COS ratio of 8/2. If total polymer concentrations are lower than 12.5 wt.%, some small "beads" are presented in nanofibers (Lee et al., 2009a). By containing MMT, PVA/COS/MMT nanocomposite nanofibers were aggregated and the homogeneity of the nanofibers was decreased. It can be concluded that, from the above discussion, the PVA/COS mass ratio and MMT content in the blend solutions are two important parameters which have remarkable effects on the morphology of electrospun sub-micron fibers of PVA/COS/MMT blend.

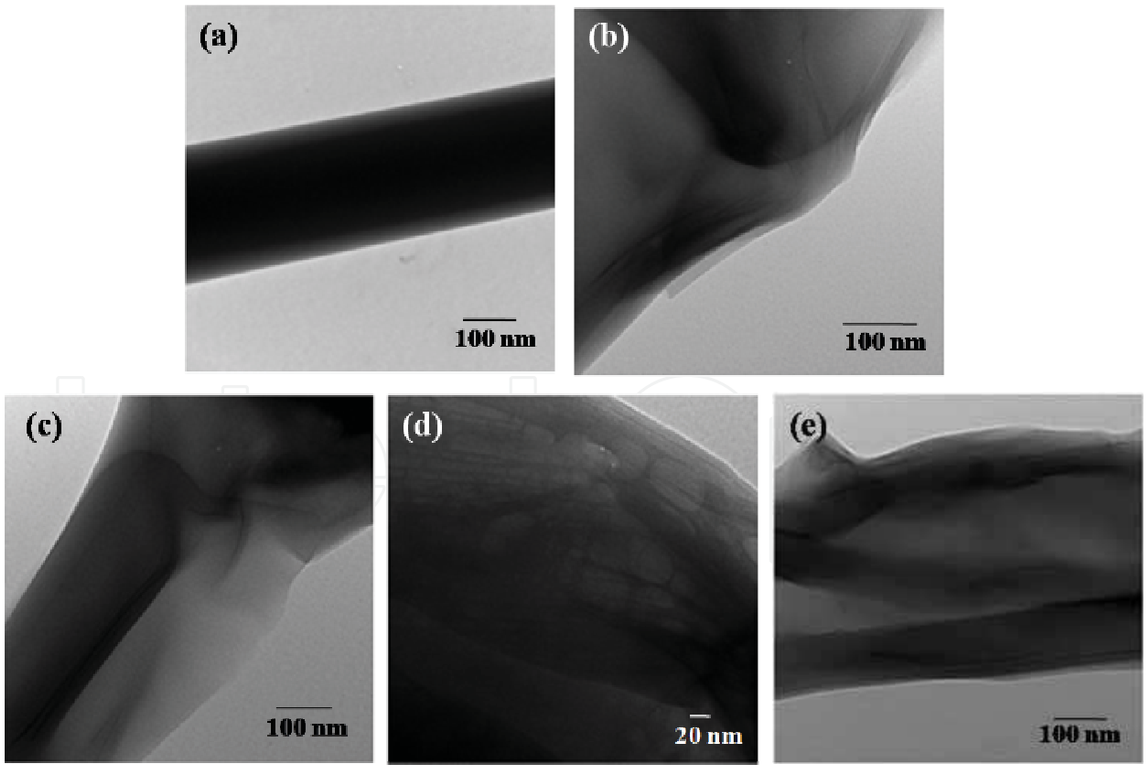

Fig. 11. TEM images of PVA/COS/MMT nanocomposite nanofibers prepared with different MMT contents of (a) 0 wt.%, (b) 1 wt.%, (c) 3 wt.%, (d) 5 wt.% and (e) 10 wt% (polymer solution concentration=12.5 wt.%, PVA/COS blend ratio=8/2)

The TEM observation reveals the formation of the nanocomposite nanofibers and the distribution of the MMT in the nanofiber matrix. The TEM image in Figure 11 indicates the nanosize MMT in the nanofibers electrospun from the solution containing 0-5 wt.% MMT. It can be clearly observed that each silicate platelet forms a dark line in the nanofiber compare with the pure PVA nanofiber.

The XRD patterns of the PVA/COS/MMT nanocomposite nanofibers are presented in Figure 12. It is well known that, in a nanoclay-polymer composite, unexfoliated or intercalated MMT usually has a peak in the range 3~9° (2θ). For exfoliated nanocomposites, on the other hand, where single silicate layers are homogeneously dispersed in the polymer matrix, and no distinct diffraction peak in the range of 3~9° (2θ) should be detected. As shown in Figure 12, as the amount of COS in the PVA/COS blend fibers is increased [(f) to (a)], the diffraction peak at about 19.3° of pristine PVA becomes broad and the intensity of the peak becomes low. Also there is no diffraction peak in 3~9° (2θ). This suggests that the crystallinity of PVA/COS fibers with higher COS amounts (8/2 and 6/4 mass ratios) is lower in comparison with the electrospun PVA fiber. TEM image (Fig. 11) also confirms that MMT clays are well dispersed in the nanofibers, and they are predominantly exfoliated.

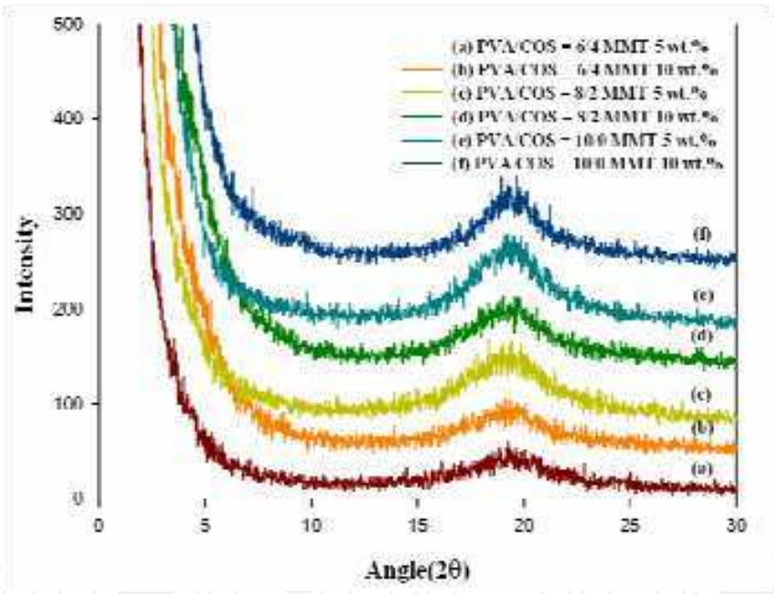

Fig. 12. XRD data of electrospun PVA/COS/MMT nanocomposite nanofibers with diffrent blend ratios and MMT contents

4.2.2 Thermal stability

Thermal stability of electrospun PVA/COS/MMT nanofiber was measured using TGA in nitrogen atmosphere. The TGA thermograms shown in Figure 13 indicate that the nanofiber mats with various PVA/COS mass ratios and MMT contents have different decomposition temperatures. All of the lines show the similar thermogram trend. However, by carefully comparison, it was found that according to mass ratio of COS and MMT, the thermal stability was changed. Higher thermal stability of high MMT content rate might be attributed from its higher chain compactness due to the interaction between the PVA and the clay.

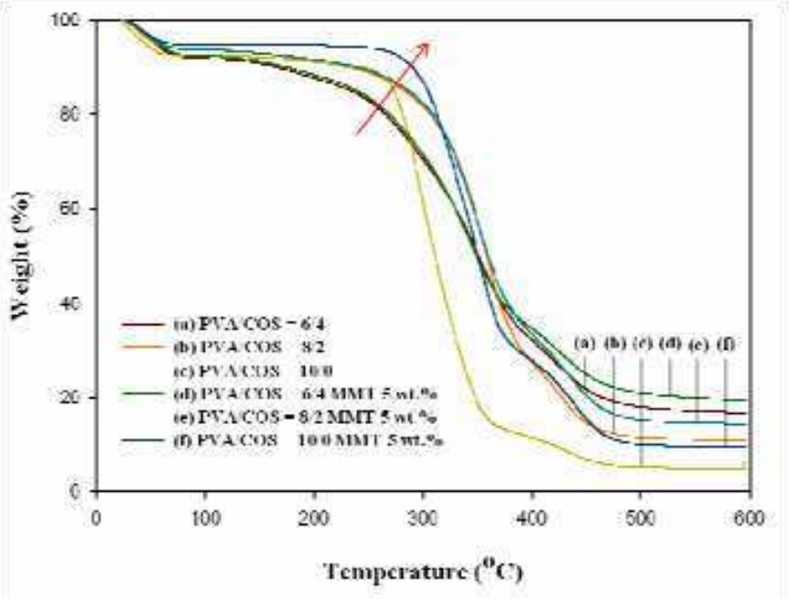

Fig. 13. TGA data of electrospun PVA/COS/MMT nanocomposite nanofibers with 0 and 5 wt.% of MMT contents (polymer solution concentration=12.5%, TCD=15 cm, and applied voltage=15 kV)

4.3 PULL/MMT nanocomposite nanofibers

4.3.1 Morphology and structure property

Both polymer and filler used in this study have hydrophilic character, the modification of MMT for component mixing was not necessary. As was described in literature (Chiellini, 2003), the solution dispersion method of PULL/clay nanocomposite preparation is often used and successful. Such method combined with vigorous stirring was also used in this work to prepare solutions for electrospinning method. Changing the polymer concentration could alter the fiber diameter and morphology very effectively. In a fixed applied voltage (15 kV) and TCD (15 cm), we used 10, 15, 20, 25, and 30 wt.% of PULL solution concentration (Karim et al., 2009). We found that at a 20 wt.% PULL concentration is ideal condition to obtain thinner and uniform PULL nanofibers. It has been obtained a nanometer range of ultrafine electrospun nanofibers (100~500 nm) in aqueous solutions as shown in Figure 14. The diameter of PULL/MMT nanofibers unaffected as well as fibers homogeneity remains identical with increasing of MMT contents from 1 to 10 wt.%. From Figure 15, TEM image supports that the coexistence of MMT clay (dark layers) and PULL matrix (light dark area) for PULL/MMT electrospun fiber mats with 5 wt.% MMT.

The spacing between clay platelets, or gallery spacing, is an indicator of the extent of intercalation/exfoliation of clay platelets within a polymer matrix and can be observed by using X-ray diffraction. Figure 16(A) shows the XRD patterns of as received PULL and MMT, and electropsun PULL/MMT nanofibers with 5 wt.% of MMT contents. Here, the XRD patterns show an intense diffraction peak in 3~9˚ for electrospun PULL/MMT nanofibers, indicating the possibility of having intercalated silicate the layers of clay dispersed in PULL matrix. There is a broad peak appearing near 19.4˚, corresponding to a d spacing of 4.52 for bulk PULL (Biliaderis et al., 1999).

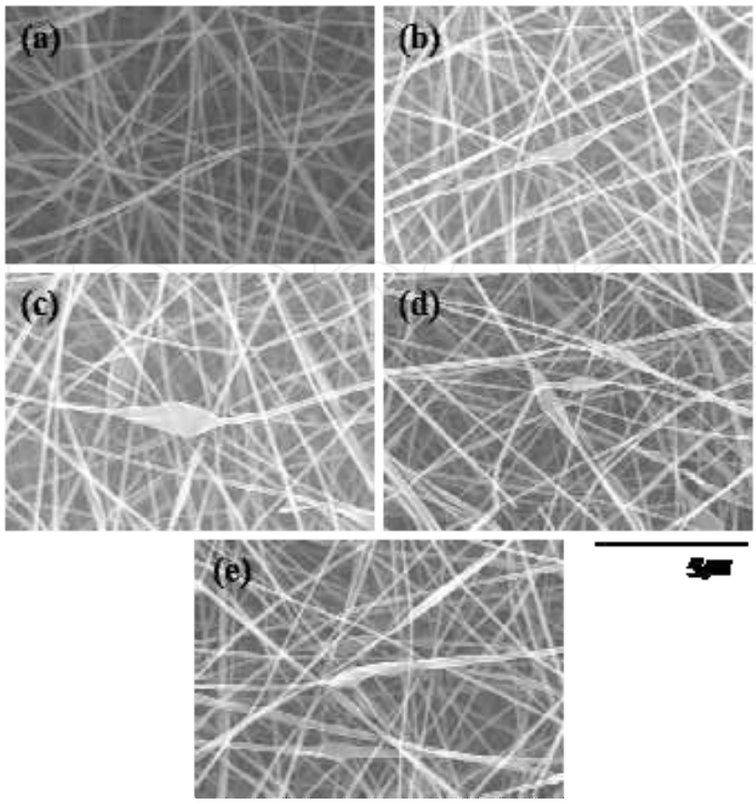

Fig. 14. FE-SEM images of PULL/MMT nanocomposite nanofibers prepared with different MMT contents of (a) 0 wt.%, (b) 1 wt.%, (c) 3 wt.%, (d) 5 wt.% and (e) 10 wt.%

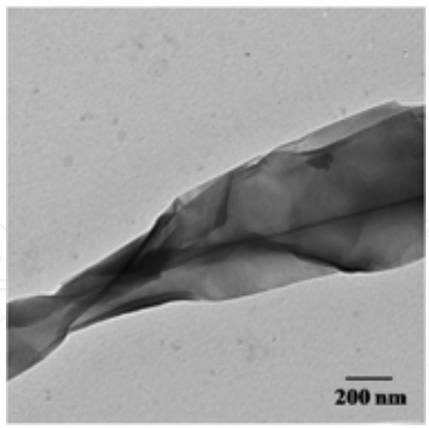

Fig. 15. TEM image of electrospun PULL/MMT nanocomposite nanofibers at 5wt.% MMT

FT-IR spectra give additional information about the structure of nanofibers studied. In Figure 16(B), examples of spectra of as received PULL powder and electrospun PULL/MMT (1, 3, 5, and 10 wt.% of MMT) nanofibers at 400–4000 cm^{-1} range are shown. Pure PULL exhibits identical bands as shown in Figure 16B(e). In the specific area (1500–650 cm^{-1}) which is characteristic for the pullulan molecule as a whole, the spectra for commercial pullulan as well as those for PULL/MMT electrospun fiber mat samples exhibited similar features. Such

results confirmed the identical chemical structure of the samples. Strong absorption in 850 cm^{-1} is characteristic of the α-D-glucopiranosid units. Absorption in 755 cm^{-1} indicates the presence of α-(1→4)-D-glucosidic bonds, and spectra in 932 cm^{-1} proved the presence of α-(1→6)-D-glucosidic bonds. Besides, in the areas for reference and evaluated samples the frequencies are analogous (Seo et al., 2004). Bands at 2850–3000 cm^{-1} are due to stretching vibrations of CH and CH_2 groups and bands attributed to CH/CH_2 deformation vibrations are present at 1300–1500 cm^{-1} range. Also very intensive, broad hydroxyl band occurs at 3000–3600 cm^{-1} and accompanying C–O stretching exists at 1000–1260 cm^{-1}. The absorption band corresponding to hydroxyl groups of PULL and MMT (3420 cm^{-1}) was reduced relative to the band of CH stretching vibrations (2930 cm^{-1}) as the interfacial interaction proceeded. Low intensive carbonyl band, is detected at 1724 cm^{-1} in PULL spectrum and gradually reduced after adding the MMT fillers. All these bands are also present in PULL composites with MMT. The small shifts of absorption maximum and alteration of band shape are results of changes in the nearest surrounding of functional groups. These observations are illustrated in Figure 16 for bands in region 1000–1750 cm^{-1}. Thus, the FT-IR spectroscopy supplied also evidences of possible interactions between PULL matrix and MMT clay, which were suggested above.

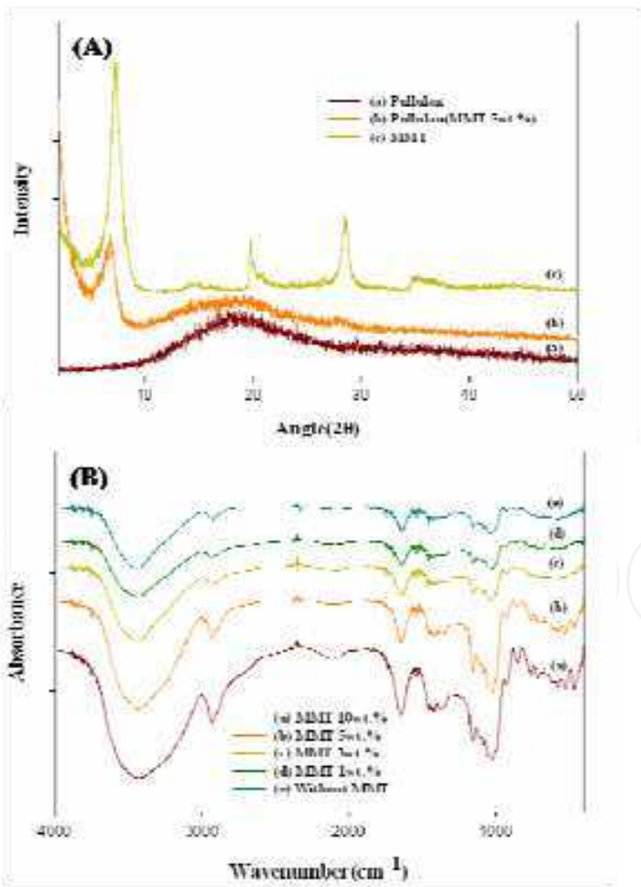

Fig. 16. (A) XRD data of as received PULL, electrospun PULL/MMT nanocomposite nanofibers and MMT (B) FT-IR data of electrospun PULL/MMT nanocomposite nanofibers with different MMT contents of (a) 10 wt.%, (b) 5 wt.%, (c) 3 wt.%, (d) 1 wt.% and (e) 0 wt.%

4.3.2 Thermal stability

The PULL/MMT nanofibers melting and crystalline point was investigated by DSC on various MMT contents. Figure 17A shows the DSC thermogram of electrospun PULL/MMT fibers with different mass of MMT contents at a polymer concentration of 20 wt.%. Pure PULL polymer showed a large thermogram peak of melting transition (T_m) at ~ 99 °C. This peak was shifted to 101.4, 102.2, 104.1, and 106.2 °C with the addition of 1, 3, 5, and 10 wt.% of MMT, respectively. The DSC for the nanofibers shows clearly the melting transitions of the PULL, in which there were significant effects of the MMT contents. It was suppressed due to the polymer confinement in accordance with previous work (Strawhecker & Manias 2000). It seems that the inorganic layer affect all polymer morphology also, even though the MMT content was still low with respect to the PULL matrix (Alla et al., 2006).

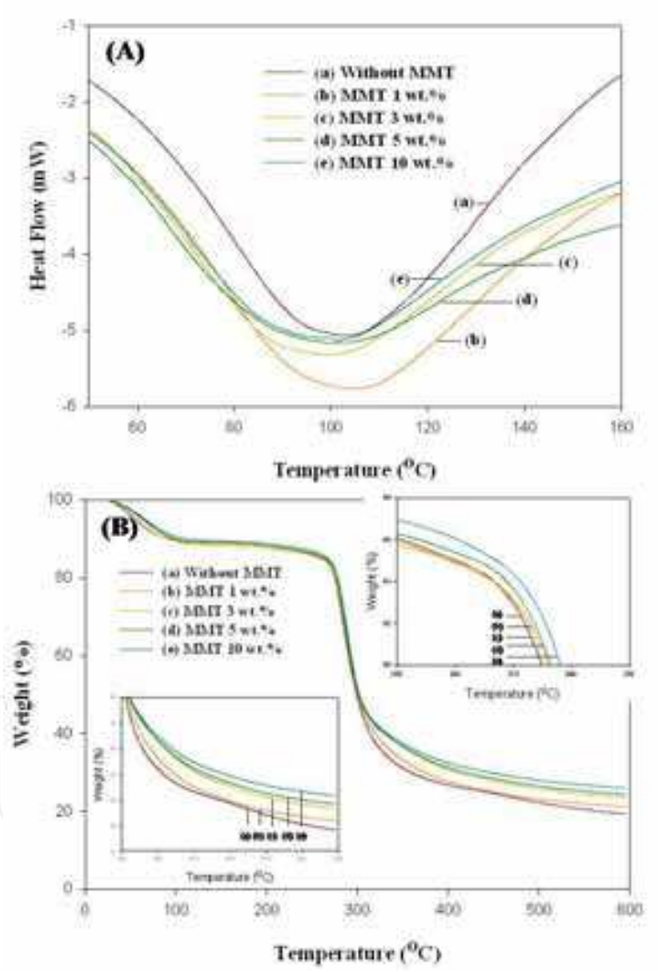

Fig. 17. (A) DSC data of electrospun PULL/MMT nanocomposite nanofibers with various MMT contents (B) TGA data of electrospun PULL/MMT nanofiber mats with different MMT contents of (a) 0 wt.%, (b) 1 wt.%, (c) 3 wt.%, (d) 5 wt.% and (e) 10 wt.%

Thermal stability of electrospun PULL/MMT nanocomposite nanofibers was measured using TGA in nitrogen atmosphere. Figure 17B shows TGA thermograms of different decomposition temperature with MMT content of 1, 3, 5, and 10 wt.%. The most below

curve of the TGA data represented the bulk PULL i.e. as received PULL powder with no MMT contents and the most upper curve was for mass ratio of 10 wt.% of MMT i.e. the highest mass ratio of MMT content was use in our work. Line (b), (c), and (d) in Figure 17B were displaying three middle mass ratios of MMT contents at the same trend of thermal stability like the line (a) and (e). Within up to 265 °C, there is increased in thermal stability from the pure PULL nanofibers to PULL/MMT (1-10 wt.%) nanocomposite nanofibers. The higher thermal stability of high MMT content rate might be attributed to its higher chain compactness due to the interaction between the PULL and the clay materials.

5. Conclusion

PVA/MMT, PVA/MMT/Ag, PVA/COS/MMT and PULL/MMT nanocomposite nanofibers with aqueous solution are successfully electrospun and characterized by FE-SEM, TEM, XRD, FT-IR, DSC and TGA. Majority of MMT platelets are exfoliated, and they are well distributed within the fiber matrix and oriented along the fiber axis. These exfoliated MMT nanoparticles improved the tensile strength and thermal stability of the electrospun nanofibers. And well dispersed Ag nanoparticles allow nanocomposite nanofibers to have a good anti-bacterial performance, which gives a suggestion for the practical use of a new preservative. The results obtained in this study may help fabricate high performance electrospun polymer nanocomposite nanofibers that can be utilized in many industries such as biomedical application, filter, reinforcement in matrix and protective clothing application.

6. Acknowledgements

This research was financially supported by the Ministry of Education Science Technology (MEST) and Korea Institute for Advancement of Technology (KIAT) through the Human Resource Training Project for Regional Innovation. Also, this work was partially supported in part by grants from the Agenda Program (PJ0073852010) of National Institute of Crop Science, Rural Development Administration (RDA), Korea.

7. References

Alla, S.G.A.; El-Din, H.M.N. & El-Naggar, A.W.M. (2006). Electron beam synthesis and characterization of poly(vinyl alcohol)/montmorillonite nanocomposites. *J Appl. Polym. Sci.*, 102, 2, 1129–1138, 0021-8995

Barber, G.D.; Calhoun, B.H. & Moore, R.B. (2005). Poly(ethylene terephthalate) ionomer based clay nanocomposites produced via melt extrusion. *Polymer*, 46, 17, 6706-6714, 0032-3861

Berkland, C.; Kim, C. & Pack, D.W. (2001). Fabrication of PLG microspheres with precisely controlled and monodisperse size distributions. *J Control. Release*, 73, 1, (18), 59-74, 0168-3659

Biliaderis, C.G.; Lazaridou, A. & Arvanitoyannis, I. (1999). Glass transition and physical properties of polyol-plasticized pullulan–starch blends at low moisture. *Carbohyd. Polym.*, 40, 1, 29–47, 0144-8617

Choi, J.S.; Lee, S.W.; Jeong, L.; Bae, S.H.; Min, B.C. & Youk, J.H. (2004). Effect of organosoluble salts on the nanofibrous structure of electrospun poly(3-

hydroxybutyrate-co-3-hydroxyvalerate). *Int. J Bio. Macromol.*, 34, 4, 249-256, 0141-8130

Farrington, J.K.; Martz, E.L.; Wells, S.J.; Ennis, C.C.; Holder, J.; Levchuk, J.W.; Avis, K.E.; Hoffman, P.S.; Hitchins, A.D. & Madden, J.M. (1995). Ability of laboratory methods to predict in-use efficacy of antimicrobial preservatives in an experimental cosmetic., *Appl. Environ. Microbiol.*, 60, 12, 4553-4558, 0099-2240

Fischer, H.R.; Gielgens, L.H. & Koster, T.P.M. (1999). Nanocomposites from polymers and layered minerals. *Acta Polym.*, 50, 4, 122-126, 0323-7648

Fleming, M.S.; Mandal, T.K. & Walt, D.R. (2001). Nanosphere−microsphere assembly: methods for core−shell materials preparation. *Chem. Mater.*, 13, 6, 2210-2216, 0897-4756

Fong, H.; Chun, I. & Reneker, D.H. (1999). Beaded nanofibers formed during electrospinning. *Polymer*, 40, 16, 4585-4592, 0032-3861

Gates, W.P.; Komadel, P.K.; Madefova, J.; Bujdak, J.; Stucki, J.W. & Kirkpatrick, R.J. (2000). Electronic and structural properties of reduced-charge maontmorillonites. *Appl. Clay Sci.*, 16, 5-6, 257-271, 0169-1317

Glaus, S.; Calzaferri, G. & Hoffmann, R. (2002). Electronic properties of the silver-silver chloride cluster interface. *Chem.-A Eur. J*, 8, 8, 1785-1794, 0947-6539

Han, X.J.; Huang, Z.M.; He, C.L.; Liu, L. & Wu, Q.S. (2006). Coaxial electrospinning of PC(shell)/PU(core) composite nanofibers for textile application. *Polym. Composite.*, 27, 4, 381-387, 0272-8397

Huang, Z.M.; Zhang, Y.Z.; Kotaki, M. & Ramakrishna, S. (2003). A review on polymer nanofibers by electrospinning and their applications in nanocomposites. *Compos. Sci. Technol.*, 63, 15, 2223-2253, 0266-3538

Israilides, C. J.; Smith, A.; Harthill, J. E.; Barnett, C.; Bambalov, G., & Scanlon, B. (1998). Pullulan content of the ethanol precipitate from fermented agro-industrial wastes. *Appl. Microbiol. Biot.*, 49, 5, 613–617, 0175-7598

Ji H.M.; Lee H.W.; Karim, M.R.; Cheong, I.W.; Bae, E.A.; Kim, T.H.; Islam M.S.; Ji, B.C. & Yeum J.H. (2009). Electrospinning and characterization of mediummolecular-weight poly(vinyl alcohol)/high-molecular-weight poly(vinyl alcohol)/montmorillonite nanofibers. *Colloid Polym. Sci.*, 287, 7, 751–758, 0303-402X

Karim, M.R.; Lee H.W.; Kim, R.; Ji B.C.; Cho J.W.; Son T.W.; Oh, W. & Yeum, J.H. (2009). Preparation and characterization of electrospun pullulan/montmorillonite nanofiber mats in aqueous solution. *Carbohyd. Polym.*, 78, 2, 336–342, 0144-8617

Kumar, A.B.V.; Varadaraj, M.C.; Lalitha, R.G. & Tharanathan, R.N. (2004). Low molecular weight chitosans: preparation with the aid of papain and characterization., *Biochim. Biophys. Acta.*, 1670, 2, 137-146, 0006-3002

Leathers, T. D. (1993). Substrate regulation and specificity of amylases from *Aureobasidium* strain NRRLY-12,974. FEMS. *Microbiology Letters*, 110, 2. 217-221, 0378-1097

Leathers, T. D. (2003). Biotechnological production and applications of Pullulan. *Appl. Microbiol. Biot.*, 62, 5-6, 468-473, 0175-7598

Lee H.W.; Karim M.R.; Park, J.H.; Ghim, H.D.; Choi, J.H.; Kim K.; Deng, Y. & Yeum, J.H. (2009a). Poly(vinyl alcohol)/chitosan oligosaccharide blend sub-micrometer fibers prepared from aqueous solutions by the electrospinning method. *J Appl. Polym. Sci.*, 111, 1, (5), 132-140, 0021-8995

Lee, H.W.; Karim, M.R.; Ji, H.M.; Choi, J.H.; Ghim, H.D.; Park, S.M.; Oh, W. & Yeum, J.H. (2009b). Electrospinning fabrication and characterization of poly(vinyl alcohol)/montmorillonite nanofiber mats. *J Appl. Polym. Sci.*, 113, 3, (5), 1860-1867, 0021-8995

Li, D. & Xia, Y. (2004). Electrospinning of nanofibers: reinventing the wheel? *Adv. Mater.*, 16, 14, 1151-1170, 0935-9648

Luna-Xavier, J.L.; Bourgeat-Lami, E. & Guyot, A. (2001). The role of initiation in the synthesis of silica/poly(methyl methacrylate) nanocomposite latex particles through emulsion polymerization. *Colloid Polym. Sci.*, 279, 10, 947-958, 0303-402X

Messersmith, P.B. & Giannelis, E.P. (1993). Polymer-layered silicate nanocomposites: in situ intercalative polymerization of epsilon.-caprolactone in layered silicates. *Chem. Mater.*, 5, 8, 1064-1066, 0897-4756

Min, B.M.; Lee, G.; Kim, S.H.; Nam, Y.S.; Lee, T.S. & Park, W.H. (2004). Electrospinning of silk fibroin nanofibers and its effect on the adhesion and spreading of normal human keratinocytes and fibroblasts in vitro. *Biomaterials*, 25, 7-8, 1289-1297, 0142-9612

Mu, L. & Feng, S.S. (2001). Fabrication, characterization and in vitro release of paclitaxel (Taxol®) loaded poly (lactic-co-glycolic acid) microspheres prepared by spray drying technique with lipid/cholesterol emulsifiers. *J Control. Release*, 76, 3, (19), 239-254, 0168-3659

Oriakhi, C.O. & Lerner, M.M. (1995). Poly(pyrrole) and poly(thiophene)/clay nanocomposites via latex-colloid interaction. *Mater. Res. Bull.*, 30, 6, 723-729, 0025-5408

Park J.H.; Karim M.R.; Kim I.K.; Cheong I.W.; Kim J.W.; Bae D.G.; Cho J.W. & Yeum, J.H. (2010). Electrospinning fabrication and characterization of poly (vinyl alcohol)/montmorillonite/silver hybrid nanofibers for antibacterial applications. *Colloid. Polym. Sci.*, 288, 1, 115–121, 0303-402X

Park, J.H.; Lee, H.W.; Chae, D.K.; Oh, W.; Yun, J.D.; Deng, Y. & Yeum, J.H. (2009). Electrospinning and characterization of poly(vinyl alcohol)/chitosan oligosaccharide/clay nanocomposite nanofibers in aqueous solutions. *Colloid Polym Sci.*, 287, 8, 943-950. 0303-402X

Reneker, D.H. & Chun, I. (1996). Nanometre diameter fibres of polymer, produced by electrospinning. *Nanotechnology*, 7, 3, 216-223, 0957-4484

Rosca, I.D.; Watari, F. & Uo, M. (2004). Microparticle formation and its mechanism in single and double emulsion solvent evaporation. *J Control. Release*, 99, 2, 271-280, 0168-3659

Rujitanaroj, P.O.; Pimpha, N. & Supaphol, P. (2008). Wound-dressing materials with antibacterial activity from electrospun gelatin fiber mats containing silver nanoparticles. *Polymer*, 49, 21, 4723-4732, 0032-3861

Sangamesh, G.K.; Syam, P.N.; Roshan, J.; Hogan, M.V. & Laurencin, C.T. (2008). Recent Patents on Electrospun Biomedical Nanostructures: An Overview. *Recent Patents Biomed. Eng.*, 1, 1, 68-78, 1874-7647

Schuster, R.; Wrenzig, E. & Mersmann, A. (1993). Production of the fungal exopolysaccharide Pullulan by batch-wise and continuous fermentation. *Appl. Microbiol. Biot.*, 39, 2, 155–158, 0175-7598

Seo, H.P.; Son, C.W.; Chung, C.H.; Jung, D.I.; Kim, S.K.; Gross, R.A. et al. (2004). Production of high molecular weight pullulan by *Aureobasidium pullulans* HP-2001 with soybean pomace as a nitrogen source. *Bioresource Technol.*, 95, 3, 293–299, 0960-8524

Strawhecker, K.E. & Manias, E. (2000). Structure and properties of poly(vinyl alcohol)/Na+ montmorillonite nanocomposites. *Chem. Mater.*, 12, 10, 2943–2949, 0897-4756

Svensson, P.D. & Staffan Hansen, S. (2010). Freezing and thawing of montmorillonite-A time-resolved synchrotron X-ray diffraction study. *Appl. Clay Sci.*, 49, 3, 127-134, 0169-1317

Tiarks, F.; Landfester, K. & Antonietti, M. (2001). Silica nanoparticles as surfactants and fillers for latexes made by miniemulsion polymerization. *Langmuir*, 17, 19, 5775-5780, 0743-7463

Usuki, A.; Kato, M.; Olada, A. & Kurauchi, T. (1997). Synthesis of polypropylene-clay hybrid. *J Appl. Polym. Sci.*, 63, 1, 137-138, 0021-8995

Vaia, R.; Vasudevan, S.; Kraweic, W.; Scanlon, L.G. & Giannelis, E.P. (1995). New polymer electrolyte nanocomposites: Melt intercalation of poly(ethylene oxide) in mica-type silicates. *Adv. Mater.*, 7, 2, 154-156, 0935-9648

Vasita, R. & Katti, D.S. (2006). Nanofibers and their applications in tissue engineering. *Int. J Nanomedicine*, 1, 1, 15-30, 1176-9114

Wang, X.; Drew, C.; Lee, S.H.; Senecal, K.J.; Kumar, J. & Samuelson, L.A. (2002). Electrospun nanofibrous membranes for highly sensitive optical sensors. *Nano Lett.*, 2, 11, 1273-1275, 1530-6984

Wu, L.L.; Yuan, X.Y. & Sheng, J. (2005). Immobilization of cellulase in nanofibrous PVA membranes by electrospinning. *J Membr. Sci.*, 250, 1-2, (15) 167-173, 0376-7388

Yeum, J.H.; Kwak, J.W.; Han, S.S.; Kim, S.S.; Ji, B.C.; Noh, S.K.; Lyoo, W.S. (2004). Water stability of high-molecular-weight (HMW) syndiotacticity-rich poly(vinyl alcohol) (PVA)/HMW atactic PVA/iodine complex blend films. *J Appl. Polym. Sci.*, 94, 4, 1435-1439, 0021-8995

Yuen, S. (1974). Pullulan and its applications. *Process Biochemistry*, 9, 7–22, 1359-5113

Zhu, J.; Wang, X.; Tao, F.; Xue, G.; Chen, T.; Sun, P.; Jin, Q. & Ding, D. (2007). Ability of laboratory methods to predict in-use efficacy of antimicrobial preservatives in an experimental cosmetic. *Polymer*, 48, 26, 7590-7597, 0032-3861

Zussmas, E.; Theron, A. & Yarin, A.L. (2003). Formation of nanofiber crossbars in electrospinning. *Appl. Phys. Lett.*, 82, 6, 973-975, 0003-6951

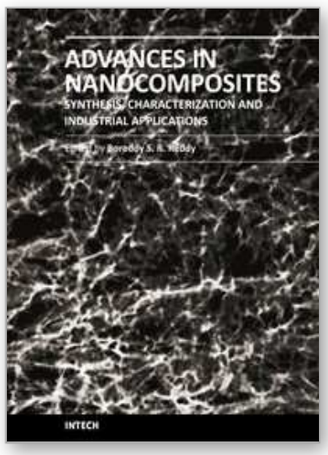

Advances in Nanocomposites - Synthesis, Characterization and Industrial Applications

Edited by Dr. Boreddy Reddy

ISBN 978-953-307-165-7
Hard cover, 966 pages
Publisher InTech
Published online 19, April, 2011
Published in print edition April, 2011

Advances in Nanocomposites - Synthesis, Characterization and Industrial Applications was conceived as a comprehensive reference volume on various aspects of functional nanocomposites for engineering technologies. The term functional nanocomposites signifies a wide area of polymer/material science and engineering, involving the design, synthesis and study of nanocomposites of increasing structural sophistication and complexity useful for a wide range of chemical, physicochemical and biological/biomedical processes. "Emerging technologies" are also broadly understood to include new technological developments, beginning at the forefront of conventional industrial practices and extending into anticipated and speculative industries of the future. The scope of the present book on nanocomposites and applications extends far beyond emerging technologies. This book presents 40 chapters organized in four parts systematically providing a wealth of new ideas in design, synthesis and study of sophisticated nanocomposite structures.

How to reference

In order to correctly reference this scholarly work, feel free to copy and paste the following:

Jeong Hyun Yeum, Jae Hyeung Park, In Kyo Kim and In Woo Cheong (2011). Electrospinning Fabrication and Characterization of Water Soluble Polymer/Montmorillonite/Silver Nanocomposite Nanofibers out of Aqueous Solution, Advances in Nanocomposites - Synthesis, Characterization and Industrial Applications, Dr. Boreddy Reddy (Ed.), ISBN: 978-953-307-165-7, InTech, Available from: http://www.intechopen.com/books/advances-in-nanocomposites-synthesis-characterization-and-industrial-applications/electrospinning-fabrication-and-characterization-of-water-soluble-polymer-montmorillonite-silver-nan

INTECH
open science | open minds

InTech Europe
University Campus STeP Ri
Slavka Krautzeka 83/A
51000 Rijeka, Croatia
Phone: +385 (51) 770 447
Fax: +385 (51) 686 166
www.intechopen.com

InTech China
Unit 405, Office Block, Hotel Equatorial Shanghai
No.65, Yan An Road (West), Shanghai, 200040, China
中国上海市延安西路65号上海国际贵都大饭店办公楼405单元
Phone: +86-21-62489820
Fax: +86-21-62489821

IntechOpen